Proceedings of the International Conference on
Formal Methods and Foundations of Artificial Intelligence
Eszterházy Károly Catholic University
Eger, Hungary, June 5–7, 2025
pp. 174–187
DOI: 10.17048/fmfai.2025.174

Physics-informed neural networks for acoustic wave propagation*

Marek Ružička, Martin Štancel, Miroslav Imrich, Dmytro Havrysh

Technical university of Košice,
Department of Computers and Informatics
{marek.ruzicka,martin.stancel,miroslav.imrich}@tuke.sk
dmytro.havrysh@student.tuke.sk

Abstract. Acoustic wave propagation plays a fundamental role in various scientific and engineering disciplines, including medical imaging, seismology, and acoustics. Traditional numerical methods such as the Finite Element Method (FEM) and Finite Difference Method (FDM) are widely used to model these waves [5, 24], but they often suffer from computational inefficiencies, especially for high-dimensional problems or complex geometries. This work explores the application of Physics-Informed Neural Networks (PINNs) as an alternative approach, leveraging deep learning to solve wave equations efficiently [14]. PINNs integrate physical laws directly into the neural network's loss function, enabling solutions that adhere to the governing differential equations. We present a comparative analysis of PINNs with traditional numerical solvers, highlighting advantages, limitations, and potential improvements. Our experiments demonstrate that PINNs can effectively model wave propagation with comparable accuracy while reducing computational cost in certain scenarios.

1. Introduction and related work

Acoustic waves play a crucial role in various fields, including engineering, medicine, geology, and many others [2]. Predicting their propagation is an important task that aids in solving diverse practical problems. However, this task is challenging

*The research was partially supported by the Slovak Academy of Sciences under Grant VEGA 1/0685/23, and partly by the Slovak Research and Development Agency under the project APVV SK-CZ-RD-21-0028.

due to the large number of factors influencing acoustic wave propagation.

PINNs [14] represent a recent direction in artificial intelligence that combines physics principles with machine learning to tackle complex problems. While traditional neural networks excel at uncovering complex data relationships, they often require extensive empirical data and may disregard the inherent physical constraints of the systems being studied. This can lead to inaccuracies or even incorrect predictions, especially where physical adherence is critical. PINNs address this by integrating physical laws as constraints directly into the network architecture and loss function, allowing the model to learn from data while respecting fundamental physics. They are particularly effective for problems described by partial differential equations (PDEs) or ordinary differential equations (ODEs).

Key benefits of PINNs include the integration of physical laws, such as conservation of mass, energy, or momentum, ensuring the correctness and reliability of predictions in physical tasks. They possess the ability to model physical processes with limited data by leveraging built-in physical principles, compensating for information scarcity. Furthermore, PINNs can be used for solving both forward and inverse problems, where unknown system parameters can be determined based on observed data. PINNs merge the statistical power of neural networks with the credibility of physical principles, providing results that are accurate and physically consistent, which is exceptionally important for scientific and engineering tasks, including the modeling of acoustic processes [11].

Acoustic wave propagation is characterized by parameters such as speed, frequency, and amplitude [28]. Key phenomena include non-linear distortion, which generates harmonics (e.g., in ultrasound), and dispersion, where wave speed varies with frequency. Dispersion is minor in gases and liquids but significant in solids due to frequency and directional dependencies. Wave interactions with obstacles involve diffraction and scattering, which are critical for modeling wave behavior in complex environments.

The use of PINNs for acoustic wave propagation prediction is still an insufficiently explored area. This work aims to investigate the possibilities of utilizing PINNs for this task. The objective is to first understand the domain of acoustic waves and analyze the current state of PINNs. Subsequently, a suitable neural network architecture and geometry will be implemented using the NVIDIA Modulus Sym environment for one-, two-, and three-dimensional problems. Experimental comparisons of various neural networks and differential operators will be conducted to identify the most effective configurations. Finally, the results will be evaluated and compared with classical numerical methods and analytical solutions. Research utilizing methods like FEM for acoustic processes, such as solving the Helmholtz equation using PINNs, has shown effectiveness in reproducing complex wave behavior in heterogeneous media and enclosed spaces with obstacles, even with minimal data and complex geometries. It has been already shown that the PINNs can improve simulation efficiency and accuracy, reducing reliance on extensive mesh generation and computational resources for wave propagation [15]. Our research specifically analyzes acoustic waves.

Recent work has begun to apply PINNs specifically to acoustic wave propagation and related audio or vibration-field problems. Yokota *et al.* [27] developed a PINN framework for acoustic resonance analysis in one-dimensional acoustic tubes, handling both forward and inverse cases to estimate energy loss terms. Schoder and Kraxberger [16] demonstrated the feasibility of solving the 3D Helmholtz equation using PINNs and benchmarked against FEM and analytic solutions, showing promise for forward acoustic modeling in spatially complex domains. Wang *et al.* [21] addressed scattered acoustic fields around complex structures via PINNs, which relates closely to modeling diffraction and obstacle interactions. Other applications include acoustic field reconstruction from limited or noisy measurements, such as in ducts or tube geometries [10], and ultrasound-based inverse problems to detect defects in media using PINNs informed by the acoustic wave equation [18]. These works illustrate both the potential and current limitations of PINNs: handling high-frequency components, enforcing absorbing or reflecting boundary conditions, computational cost in 3D, and robustness under noisy or partial observation.

2. Definition of PINN

PINNs are deep learning models that integrate known physical laws, typically expressed as PDEs or ODEs, into the training process to ensure that the model's predictions adhere to the underlying physics [14]. PINNs consist of three primary components: a neural network that approximates the solution of a physical system, a set of differential equations representing the physical laws governing the system, and a loss function that penalizes deviations from both observed data and physical consistency. The neural network, commonly implemented as a multilayer perceptron (MLP), approximates a target function $u(x)$ with $u_\theta(x)$, where θ denotes the model parameters such as weights and biases [4]. These networks typically employ activation functions like *tanh* or $ReLU$, with a preference for differentiable functions to facilitate effective gradient-based optimization.

To embed physical principles into the model, PINNs include the governing equations directly into the loss function. Instead of relying on numerical solvers, the network learns to satisfy physical constraints by minimizing the error induced by these equations [14]. This approach enables PINNs to generalize from limited data while maintaining physical plausibility.

Physical constraints can be introduced in two main ways. First, physical parameters, such as wave speed, pressure, or medium density, can be included as additional features in the input. This helps the network better model spatial or temporal dependencies, particularly in dynamic systems like acoustic waves [7]. Second, the physical equations themselves can be encoded into the loss function, ensuring that the learned solution remains consistent with the physics throughout the domain. The total loss function $L(\theta)$ used to train a PINN is composed of two parts: a data loss term $L_{\text{data}}(\theta)$ that measures the discrepancy between model predictions and available measurements, and a physics loss term $L_{\text{physics}}(\theta)$ that penalizes violations of the governing physical laws [14]:

$$L(\theta) = L_{\text{data}}(\theta) + L_{\text{physics}}(\theta)$$

3. Theorem

Let $N(u)$ represent a differential operator derived from the physical law such that the governing equation is $N(u) = 0$. The physics loss term can then be defined as the mean squared error of the residual evaluated at M collocation points $\{x_j\}_{j=1}^{M}$ [14]:

$$L_{\text{physics}}(\theta) = \frac{1}{M}\sum_{j=1}^{M} |N(u_\theta(x_j))|^2$$

This term ensures that the network's outputs not only fit the data but also satisfy the physical constraints within the problem domain [3, 6]. The relative weight between the data and physics losses can be adjusted adaptively to improve training stability and accuracy.

Training involves minimizing the total loss function using optimization algorithms such as gradient descent, Adam, or L-BFGS. Additionally, techniques such as adaptive sampling, weighting strategies, and residual-based refinement can improve convergence, especially when solving stiff or ill-posed problems [11].

Beyond forward modeling, PINNs can also solve inverse problems, such as identifying unknown parameters or reconstructing missing input data from limited measurements [14]. Regularization strategies, including activation function tuning and weighted residuals, can enhance accuracy. The spatial distribution of training points, whether uniform, random, or adaptive, also influences model performance [23].

To evaluate a PINN's accuracy and physical validity, standard metrics such as Mean Absolute Error (MAE), Mean Squared Error (MSE), Root Mean Squared Error (RMSE), and the L_2 norm are commonly used [14, 22]. Adherence to conservation laws, like mass or energy conservation, further confirms the reliability of the model [6, 20, 23].

While traditional PINNs rely on fully connected MLPs, alternative architectures such as Convolutional Neural Networks (CNNs) and Recurrent Neural Networks (RNNs) have been employed to better handle spatial and temporal dependencies [3, 4, 17]. Recently, Bayesian extensions of PINNs (B-PINNs) have emerged as a promising approach for uncertainty quantification in scenarios where prediction reliability is critical [25].

4. Application of PINNs to wave problems

The wave equation is a fundamental equation in mathematical physics, describing a wide range of wave processes from 1D string vibrations to 2D membrane oscillations and 3D acoustic waves. The core idea remains the same regardless of dimension: examining the dynamics of a wave propagating through a medium, reflecting from boundaries, or interacting with them. PINNs were applied to wave problems of different dimensions within the NVIDIA Modulus Sym environment.

The NVIDIA Modulus Sym framework is a specialized tool designed for modeling physical processes using PINNs. It supports GPU optimization for high computational efficiency, crucial for large-scale simulations [12]. Modulus offers built-in support for physical equations like the Helmholtz equation for acoustics and provides tools for creating and training PINNs by including physical constraints in the loss functions. While general frameworks like TensorFlow and PyTorch can implement PINNs, Modulus provides specialized tools for handling physical equations, which might require manual configuration in the others [1, 13]. Modulus allows control over simulations via configuration files, specifying training parameters, network architecture, equations, domains, and constraints.

Key advantages of NVIDIA Modulus include its optimization for NVIDIA GPUs, enabling significantly faster model training for large-scale physical simulations [12]. It features integrated tools for working with physical laws and equations, simplifying the creation of complex models with physical constraints, including the Helmholtz equation for acoustics. Modulus also provides ready-made templates and examples for various physical tasks. Disadvantages include its dependence on NVIDIA GPU hardware and the requirement for prior experience with GPUs and physical process modeling for setup and use.

We have applied PINNs to three wave problems. 1D Wave Equation with Fixed Boundaries is defined as:

$$\frac{\partial^2 u}{\partial t^2} = c^2 \frac{\partial^2 u}{\partial x^2}$$

The PINN was trained to simultaneously satisfy the initial conditions $u(x, 0)$ and $\partial u/\partial t$ at $t = 0$, boundary conditions $u = 0$ at $x = 0$ and $x = L$, and the differential equation itself via a residual term [14]. c represents the wave speed. A fully connected MLP was used, taking (x, t) as input and outputting $u(x, t)$. Parameters like layer count and size were configurable. An example comparison with an analytical solution is shown in Figure 1.

2D equation extends to two spatial dimensions (x, y):

$$\frac{\partial^2 u}{\partial t^2} = c^2 \left(\frac{\partial^2 u}{\partial x^2} + \frac{\partial^2 u}{\partial y^2} \right)$$

This equation can describe, for example, membrane oscillations or other 2D wave processes. The same overall PINN scheme was used as in the 1D case, but network parameters were adjusted for increased complexity. A fully connected architecture was retained, with an increased layer size (256 neurons) to accommodate the 2D task's complexity. Optimizer details (Adam, learning rate, exponential decay) were specified.

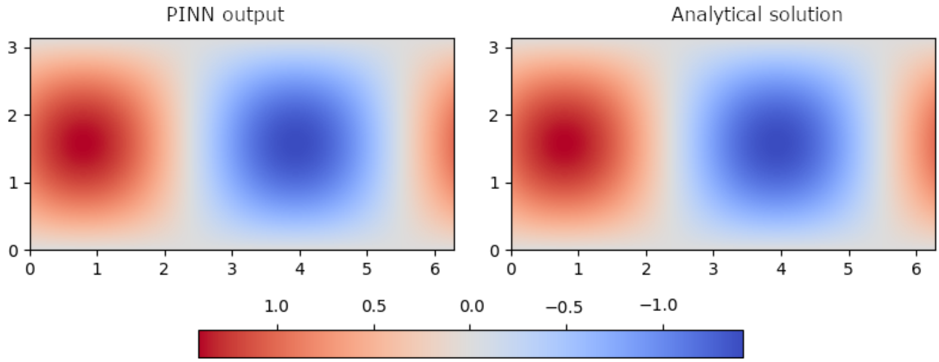

Figure 1. Comparison of PINN prediction with analytical solution.

Finally, 3D equation includes a third spatial dimension (z):

$$\frac{\partial^2 u}{\partial t^2} = c^2\left(\frac{\partial^2 u}{\partial x^2} + \frac{\partial^2 u}{\partial y^2} + \frac{\partial^2 u}{\partial z^2}\right)$$

The simulation area was a cube. Initial conditions defined a harmonic function dependent on all three spatial coordinates, starting from rest. Zero displacement boundary conditions were applied on all six faces, simulating a fixed membrane. This configuration creates a complex interference pattern [12]. The same network architecture and hyperparameters as the 2D case were used for direct comparison of convergence and solution accuracy. A static cross-section visualizing the displacement field at a specific time slice showed solution symmetry and reflections from fixed walls, as seen in Figure 2.

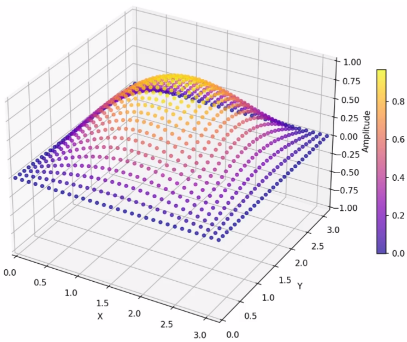

Figure 2. Visualization the three-dimensional wave equation.

Additionally, 2D wave equation with Perfectly Matched Layers (PML) and Obstacle was implemented. This complex case involved a 2D area with a circular obstacle and surrounding PML [28]. PML is a numerical technique to absorb waves and simulate open boundaries, preventing unwanted reflections in wave process simulations like acoustic, electromagnetic, or elastic waves. It absorbs wave energy before it reaches the outer edge, simulating open space. The governing equations become a system involving the acoustic pressure and auxiliary fields to ensure absorption. A Neumann boundary condition $\partial u/\partial n = 0$ was applied on the obstacle's surface, simulating a perfectly rigid body reflecting waves [8]. Numerically, this condition is evaluated using components of the normal vector. The PINN formulation uses symbolic description of geometry, allowing precise application of boundary conditions on the curved surface by computing the normal using symbolic expressions [12]. An initial Gaussian pulse was defined. The network predicted the primary field (u), auxiliary PML fields (ψ_x, ψ_y), and additional quantities for normal derivatives. Due to the high complexity (multiple unknown functions, geometry, PML), optimizing the training process was necessary. An initial issue with GPU memory exceeding limits was resolved by halving the batch size, allowing training to complete with sufficient accuracy. Figure 3 shows the time evolution of the wave in this scenario.

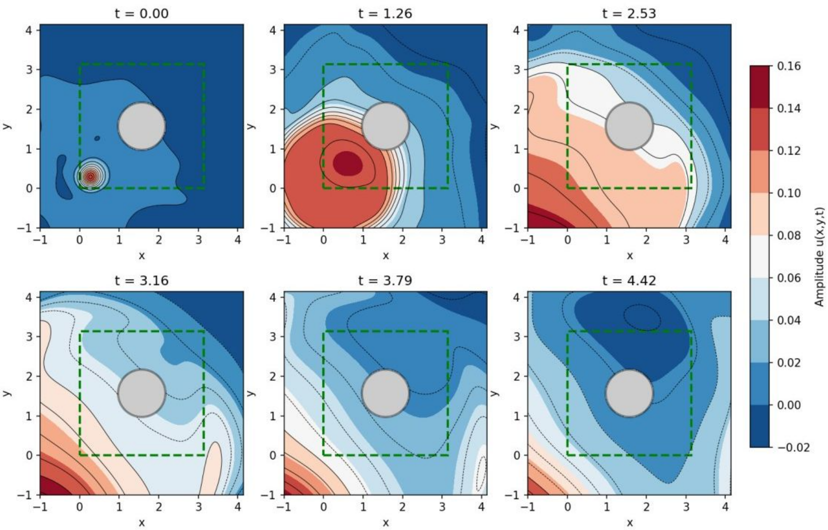

Figure 3. Time evolution of the acoustic wave in an area with an obstacle and absorbing PML.

Implementing these models in Modulus Sym involves defining the physics equations, specifying the geometry and boundary/initial conditions, configuring the neural network architecture and training parameters using YAML files, and setting up constraints and inferencers.

To model the underlying physical system, we employed a fully connected neural network using the Modulus Sym framework. The network architecture is designed to approximate the solution to a spatiotemporal problem by taking spatial coordinates (x, y) and time t as input variables, and producing a scalar output p, representing the target physical quantity (e.g., pressure).

The network consists of five hidden layers, each containing 128 neurons. The activation function used across all layers is the hyperbolic tangent (*tanh*), which is commonly chosen for its smooth differentiability and favorable gradient properties when solving differential equations. The architecture is implemented using the FullyConnectedArch module in Modulus Sym, and is parameterized with appropriately defined symbolic input and output keys to facilitate automatic differentiation and integration with physics-informed loss functions.

To evaluate the predictive performance of the trained model, several error metrics were computed by comparing the predicted values p_{pred} with the reference data p_{ref} [22]. The element-wise difference between predicted and true values was first computed as $\Delta p = p_{\text{pred}} - p_{\text{ref}}$. Based on this difference, the following statistical indicators were calculated:

MSE: Computed as the average of the squared differences, it quantifies the mean magnitude of the prediction errors,

$$\text{MSE} = \frac{1}{N}\sum_{i=1}^{N}(\Delta p_i)^2.$$

RMSE: Defined as the square root of the MSE, providing an interpretable error magnitude in the same units as the output variable,

$$\text{RMSE} = \sqrt{\text{MSE}}.$$

Mean Error: The average of the raw differences between predicted and reference values,

$$ME = \frac{1}{N}\sum_{i=1}^{N}(p_{\Delta p_i}).$$

These metrics provide a comprehensive evaluation of model accuracy, consistency, and the nature of deviations from the true solution.

The quality of the obtained solutions was evaluated for all analyzed cases, from the basic 1D model to the most complex task with an obstacle and absorbing PML. The main objective was to verify the physical correctness of PINN predictions, compare results with reference solutions (analytical or numerical), and assess PINNs' ability to solve problems with complicated geometries and absorbing boundaries.

5. Results

Comparisons with analytical and FDM solutions for the 1D case showed very good agreement. Heat maps and wave profiles demonstrated minimal deviations. Quantitative metrics (MSE, L2-norm) were low (e.g., MSE of 1×10^{-6} vs. analytical, 6.7×10^{-5} vs. FDM for 1D; MSE of 5.437×10^{-7} vs. analytical, 5.347×10^{-7} vs. FDM for 2D; MSE of 6.256×10^{-6} vs. analytical, 6.253×10^{-6} vs. FDM for 3D). PINNs successfully captured the dynamics of wave propagation with fixed boundaries in all dimensions. This confirmed PINNs' suitability for these academic examples and their ability to provide accurate solutions comparable to traditional methods like FDM. A key advantage highlighted was that PINNs do not require explicit mesh discretization [14]. In practical terms, the reported errors correspond to sub-percent deviations in wave amplitude, which are sufficient for engineering analysis where qualitative propagation patterns dominate. The accuracy achieved in 3D was sufficient for practical applications in complex configurations. As can be seen in the visualization in Figure 4, in the 3D wave case, the difference between the prediction and the analytical solution is minimal. In 1D and 2D cases, the error is so low that it can't be spotted visually. These results illustrate the robustness of PINNs for lower-dimensional problems and their potential as mesh-free solvers for higher dimensions, although the computational effort increases significantly compared to FDM. From the theoretical standpoint, the small residuals confirm that the physics loss term effectively constrained the solution across collocation points.

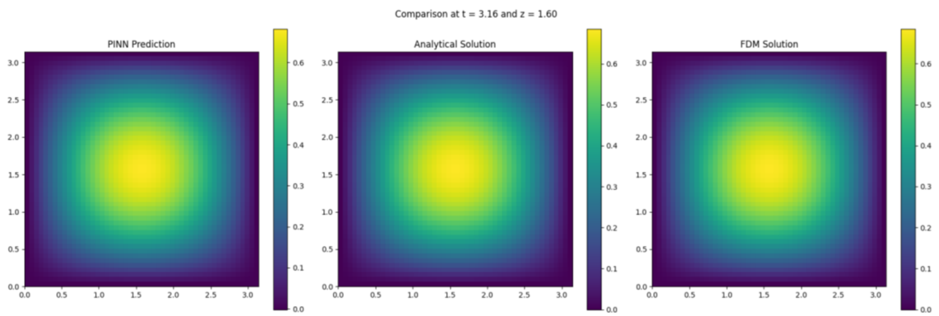

Figure 4. Comparison of FDM, PINN output and analytical solution for 3D wave at $z \approx 0$.

2D Acoustic Wave with Object and PML case was analyzed in parts: initial Gaussian pulse propagation, interaction with an obstacle, and absorption by PML.

Comparison of Gaussian Pulse in 2D without obstacle/PML with FDM showed acceptable accuracy. Visual differences were observed, particularly on the wave front. Quantitative metrics like relative L2 error were higher (8.2712×10^{-1}) compared to the simpler 1D/2D/3D cases. The relatively high error indicates that while PINNs can capture the main wave structure, sharp gradients and high-frequency components remain challenging, especially in higher-dimensional problems. Increasing network parameters improved accuracy but also slightly increased wave amplitude, indicating sensitivity to hyperparameters. Such behavior highlights a limitation of PINNs: their performance is strongly tied to architecture choices and may require extensive tuning, unlike FDM which has more predictable convergence behavior. Finding a closed-form analytical solution for a Gaussian pulse in 2D is challenging due to non-linearity and the need for complex functions like Bessel functions. The difficulty in this case reflects the challenge of minimizing $N(u_\theta(x_j))$

near steep gradients, where the residual term dominates the loss.

PINNs utilize a precise symbolic description of the circular obstacle geometry and boundary condition application [26]. Differences observed when comparing PINN results with FDM/FEM solutions are attributed primarily to the PINN's precise handling of the curved boundary condition via symbolic computation of the normal, contrasting with the approximate nature of this condition in FDM/FEM [3]. Such accuracy is particularly relevant in scenarios where faithful representation of curved or irregular boundaries is critical, such as biomedical or seismic wave simulations. Other sources of difference include numerical approximations in classical methods and potential discrepancies in initial impulse definition or time parameters. Aligning results requires more accurate boundary condition methods in classical techniques (e.g., immersed boundary, body-fitted mesh) and careful matching of initial and boundary conditions and discretization. A fundamental difference remains in how the solution is obtained: PINN optimizes a functional with analytical geometry, while FDM/FEM solve a discretized equation with precision limited by the discrete mesh [14]. The functional approach also enables PINNs to generalize solutions at arbitrary collocation points, whereas traditional methods are tied to predefined meshes. This observation directly illustrates the theoretical advantage of embedding the operator $N(u)$ in the loss: boundary conditions are enforced analytically rather than approximated numerically.

Comparison of PINN and FDM solutions of absorption in PML showed good overall approximation by PINN, but minor artifacts appeared in the upper region. These artifacts could potentially be due to imprecise PML boundary conditions in the PINN model. FDM showed clearer wave propagation. Quantitative errors; MSE=0.00321, RMSE=0.00545, with maximum error for a single collocation point 0.0213; indicated a small average deviation but significant local deviations on the wave front, suggesting PINNs' sensitivity to steep gradients. Such sensitivity limits their use in problems where sharp wavefront accuracy is critical (e.g., shock waves), unless specialized loss functions or adaptive sampling strategies are employed. The PML implementation in PINN showed artifacts, indicating it did not perfectly absorb waves, possibly due to suboptimal boundary condition setup in the loss function or architecture limitations. Further optimization was limited by computational resources. The growing training cost with domain complexity represents another limitation, which may offset the benefits of mesh-free formulation in large-scale 3D applications. From the perspective of the theorem, these artifacts indicate incomplete minimization of the residual at collocation points near the absorbing boundary, pointing to a need for refined loss weighting.

Three different neural network architectures were implemented for the 2D wave equation with PML and an object: Fully Connected, Fourier Neural Operator (FNO), and SIREN [3, 4, 9, 19]. Hyperparameters were kept the same across all cases for comparison, thus 5 layer network, 128 neurons per layer and tanh activation function for fully connected neural net and default Modulus values for FNO and SIREN.

The Fully Connected architecture yielded the best and most stable results among those tested with the given configuration. It demonstrated smoother convergence and physically more correct wave behavior in the impulse problem. Classical dense architectures therefore remain a competitive baseline for wave problems, especially when training resources are constrained.

The FNO architecture showed a high initial loss that decreased rapidly in the first thousands of iterations, then settled at a lower level. This suggests FNO finds the main frequency components relatively quickly, but the solution was not completely ideal regarding reflection and absorption. Parameter tuning (normalization, number of harmonics) improved FNO results, reducing noise and yielding a recognizable impulse, but still not fully physically correct propagation, reflection, or absorption, see Figure 5. The gray circle represents an obstacle and the green square represents PML. These observations highlight both the promise of operator learning approaches for capturing global patterns, and their current limitations in faithfully reproducing fine-scale boundary interactions without tailored architectures.

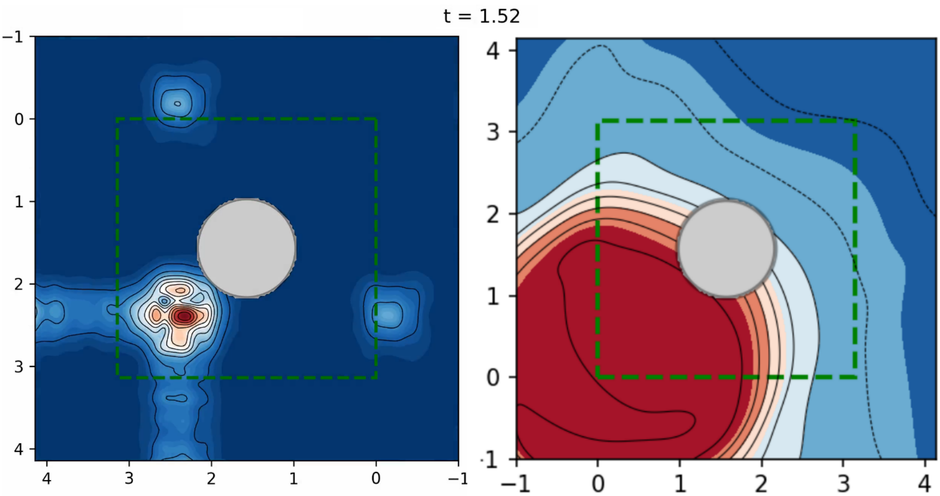

Figure 5. Result of the FNO model (left) after parameter optimization and Fully Connected (right) at the same time.

The SIREN architecture started with a very high loss and decreased slowly, remaining at a significantly higher value than the other architectures. The model struggled to find a sufficiently good representation of the wave field. For impulse disturbances with a wide frequency spectrum, SIREN typically requires special initialization techniques and frequency scaling. While SIRENs are powerful for high-frequency representations, their application to broadband wave propagation remains limited without problem-specific adaptations.

In summary, the results demonstrate that PINNs can achieve accuracy comparable to FDM and FEM in structured wave problems, with clear benefits in handling curved geometries and mesh-free generalization. However, their practical deployment is limited by high computational cost, sensitivity to hyperparameters, and challenges with absorbing boundaries or sharp gradients. PINNs are therefore most promising for problems where geometric flexibility and smooth solutions are more critical than computational efficiency, such as biomedical or geophysical applications. Overall, the experiments confirm the theoretical formulation: minimizing the total loss $L(\theta) = L_{\text{data}} + L_{\text{physics}}$ produces solutions that not only fit data but also satisfy the governing PDE residuals within the domain.

6. Conclusion

This study investigated the application of PINNs for acoustic wave propagation prediction. A theoretical overview of acoustic waves and the PINN approach was provided, followed by simulations in NVIDIA Modulus Sym for one-, two-, and three-dimensional cases, including absorbing boundaries and rigid obstacles.

PINNs modeled wave phenomena in open boundaries and complex geometries without explicit space–time discretization, a key advantage over classical numerical methods. However, the models were sensitive to training parameters, especially in complex configurations (e.g., with impulse disturbances and PML), where artifacts, amplitude reduction, or wavefront deformation appeared. These issues arose from loss-function setup, excessive weighting of boundaries, uneven collocation points, or low weights in the interior domain.

Comparison with analytical, FDM, and FEM solutions confirmed the advantage of PINNs in applying boundary conditions to curved geometries via symbolic description. While accuracy was not uniform across the entire domain, PINNs generally preserved the physical structure of the solution and reproduced key wave properties.

Among Fully Connected, FNO, and SIREN architectures, the classical fully connected network yielded the most stable and physically correct results, emphasizing that architecture choice should reflect the disturbance type and expected solution form.

Although training is computationally intensive, PINNs' flexibility, mesh-free formulation, and incorporation of physical laws make them a promising tool for modeling complex physical processes. Future work should expand to more architectures, improve sampling strategies, and apply regularization to enhance accuracy, particularly for impulse waves and absorbing layers.

References

[1] M. Abadi, A. Agarwal, P. Barham, E. Brevdo, Z. Chen, C. Citro, G. S. Corrado, A. Davis, J. Dean, M. Devin, et al.: *Tensorflow: Large-scale machine learning on heterogeneous distributed systems*, arXiv preprint arXiv:1603.04467 (2016).

[2] J. Brum: *Transverse wave propagation in bounded media*, Ultrasound elastography for biomedical applications and medicine (2018), pp. 90–104.

[3] S. Cai, Z. Mao, Z. Wang, M. Yin, G. E. Karniadakis: *Physics-informed neural networks (PINNs) for fluid mechanics: A review*, Acta Mechanica Sinica 37 (2021), pp. 1727–1738, doi: 10.1007/s10409-021-01148-1.

[4] K. Gurney: *An Introduction to Neural Networks*, Boca Raton, FL, USA: CRC Press, 2018.

[5] Y. Kagawa, T. Tsuchiya, T. Yamabuchi, H. Kawabe, T. Fujii: *Finite element simulation of non-linear sound wave propagation*, Journal of sound and vibration 154.1 (1992), pp. 125–145.

[6] G. E. Karniadakis, I. G. Kevrekidis, L. Lu, P. Perdikaris, S. Wang, L. Yang: *Physics-informed machine learning*, Nature Reviews Physics 3 (2021), pp. 422–440, doi: 10.1038/s42254-021-00314-5.

[7] S. W. Kim, I. Kim, J. Lee, S. Lee: *Knowledge Integration into deep learning in dynamical systems: An overview and taxonomy*, Journal of Mechanical Science and Technology 35 (2021), pp. 1331–1342.

[8] L. E. Kinsler, A. R. Frey, A. B. Coppens, J. V. Sanders: *Fundamentals of Acoustics*, 4th ed., John Wiley & Sons, 2000.

[9] Z. Li, N. Kovachki, K. Azizzadenesheli, B. Liu, K. Bhattacharya, A. Stuart, A. Anandkumar: *Fourier neural operator for parametric partial differential equations*, arXiv preprint arXiv:2010.08895 (2020).

[10] X. Luan, K. Yokota, G. Scavone: *Acoustic field reconstruction in tubes via physics-informed neural networks*, arXiv preprint arXiv:2505.12557 (2025).

[11] N. Mehtaj, S. Banerjee: *Scientific machine learning for guided wave and surface acoustic wave (SAW) propagation: PgNN, PeNN, PINN, and neural operator*, Sensors (Basel, Switzerland) 25.5 (2025), p. 1401.

[12] NVIDIA Corporation: *NVIDIA Modulus: Physics-Informed Neural Networks Framework*, https://developer.nvidia.com/modulus, 2024.

[13] A. Paszke: *Pytorch: An imperative style, high-performance deep learning library*, arXiv preprint arXiv:1912.01703 (2019).

[14] M. Raissi, P. Perdikaris, G. E. Karniadakis: *Physics-informed neural networks: A deep learning framework for solving forward and inverse problems involving nonlinear partial differential equations*, Journal of Computational physics 378 (2019), pp. 686–707.

[15] M. Rasht-Behesht, C. Huber, K. Shukla, G. E. Karniadakis: *Physics-informed neural networks (PINNs) for wave propagation and full waveform inversions*, Journal of Geophysical Research: Solid Earth 127.5 (2022), e2021JB023120.

[16] S. Schoder, F. Kraxberger: *Feasibility study on solving the Helmholtz equation in 3D with PINNs*, arXiv preprint arXiv:2403.06623 (2024).

[17] A. Sherstinsky: *Fundamentals of recurrent neural network (RNN) and long short-term memory (LSTM) network*, Physica D: Nonlinear Phenomena 404 (2020), p. 132306, doi: 10.1016/j.physd.2019.132306.

[18] K. Shukla, P. C. Di Leoni, J. Blackshire, D. Sparkman, G. E. Karniadakis: *Physics-informed neural network for ultrasound nondestructive quantification of surface breaking cracks*, Journal of Nondestructive Evaluation 39.3 (2020), p. 61.

[19] V. Sitzmann, J. Martel, A. Bergman, D. Lindell, G. Wetzstein: *Implicit neural representations with periodic activation functions*, Advances in neural information processing systems 33 (2020), pp. 7462–7473.

[20] L. Sun, H. Gao, S. Pan, J. X. Wang: *Surrogate modeling for fluid flows based on physics-constrained deep learning without simulation data*, Computational Methods in Applied Mechanics and Engineering 361 (2020), p. 112732, doi: 10.1016/j.cma.2019.112732.

[21] H. Wang, J. Li, L. Wang, L. Liang, Z. Zeng, Y. Liu: *On acoustic fields of complex scatters based on physics-informed neural networks*, Ultrasonics 128 (2023), p. 106872.

[22] Q. Wang, Y. Ma, K. Zhao, Y. Tian: *A comprehensive survey of loss functions in machine learning*, Annals of Data Science 9.2 (2022), pp. 187–212.

[23] S. Wang, Y. Teng, P. Perdikaris: *Understanding and mitigating gradient flow pathologies in physics-informed neural networks*, SIAM Journal on Scientific Computing 43.5 (2021), https://arxiv.org/abs/2001.04536, A3055–A3081.

[24] H. Yamawaki, T. Saito: *Computer simulation of acoustic waves propagation in elastically anisotropic materials*, in: Materials Science Forum, vol. 210, Trans Tech Publ, 1996, pp. 589–596.

[25] L. Yang, X. Meng, G. E. Karniadakis: *B-PINNs: Bayesian physics-informed neural networks for forward and inverse PDE problems with noisy data*, Journal of Computational Physics 425 (2021), p. 109913, doi: 10.1016/j.jcp.2020.109913.

[26] Y. Yang, P. Perdikaris, G. E. Karniadakis: *Physics-informed deep learning for the nonlinear dynamics of materials*, Computer Methods in Applied Mechanics and Engineering 389 (2022), p. 114378, doi: 10.1016/j.cma.2021.114378.

[27] K. Yokota, T. Kurahashi, M. Abe: *Physics-informed neural network for acoustic resonance analysis in a one-dimensional acoustic tube*, The Journal of the Acoustical Society of America 156.1 (2024), pp. 30–43.

[28] S. Yoshida: *Fundamentals of Acoustic Waves and Applications*, Springer, 2024.